

---

# TRANSFER LEARNING AND LOCAL INTERPRETABLE MODEL AGNOSTIC BASED VISUAL APPROACH IN MONKEYPOX DISEASE DETECTION AND CLASSIFICATION: A DEEP LEARNING INSIGHTS

---

A PREPRINT

**Md Manjurul Ahsan**

Department of Industrial and Systems Engineering  
University of Oklahoma  
Norman, Oklahoma-73071  
ahsan@ou.edu

**Tareque Abu Abdullah**

Department of Computer Science  
Lamar University  
Beaumont, TX-77710  
tabdullah@lamar.edu

**Md Shahin Ali**

Department of Biomedical Engineering  
Islamic University  
Kushtia-7003, Bangladesh  
shahin@std.iu.ac.bd

**Fatematuj Jahora**

Child Development and Social Relationship  
Government College of Applied Human Science  
Azimpur, Dhaka-1205, Bangladesh  
fatema.cdsr@gmail.com

**Md Khairul Islam**

Department of Biomedical Engineering  
Islamic University  
Kushtia-7003, Bangladesh  
khairul@bme.iu.ac.bd

**Amin G. Alhashim**

Department of Industrial and systems Engineering  
Arizona State University  
7271 E. Sonoran Arroyo Mall Mesa, AZ-85212  
alhashim.asu@gmail.com

**Kishor Datta Gupta**

Department of Computer and Information Science  
Clark Atlanta University  
Atlanta, GA-30314, USA  
kgupta@cau.edu

November 16, 2022

## ABSTRACT

The recent development of Monkeypox disease among various nations poses a global pandemic threat when the world is still fighting Coronavirus Disease-2019 (COVID-19). At its dawn, the slow and steady transmission of Monkeypox disease among individuals needs to be addressed seriously. Over the years, Deep learning (DL) based disease prediction has demonstrated true potential by providing early, cheap, and affordable diagnosis facilities. Considering this opportunity, we have conducted two studies where we modified and tested six distinct deep learning models—VGG16, Inception-ResNetV2, ResNet50, ResNet101, MobileNetV2, and VGG19—using transfer learning approaches. Our preliminary computational results show that the proposed modified InceptionResNetV2 and MobileNetV2 models perform best by achieving an accuracy ranging from 93% to 99%. Our findings are reinforced by recent academic work that demonstrates improved performance in constructing multiple disease diagnosis models using transfer learning approaches. Lastly, we further explain our model prediction using Local Interpretable Model-Agnostic Explanations (LIME), which plays an essential role in identifying important features that characterize the onset of Monkeypox disease.

**Keywords** Convolutional neural network · Deep learning · Disease diagnosis · Image processing · Monkeypox · Transfer learning

## 1 Introduction

Monkeypox, also known as Monkeypox Virus (MPXV) disease, is caused by infection with the virus of the same name and is usually found in monkeys [1]. Monkeypox usually occurs in Africa, Central and West Africa, and Asia [2]. Although it can infect any mammal, the virus spreads to humans primarily through the bite of an infected animal like a bat or primate such as a monkey [3]. There are several early monkeypox symptoms, including muscle pain, headache, fatigue, and fever. The disease almost resembled chickenpox, smallpox, and measles. It can be distinguished from the appearance of swollen glands, usually present behind the ear, below the jaw, neck, or groin, before the onset of the rash [4]. Even though the virus is not life-threatening, it causes complications in severe cases, including sepsis, pneumonia, and loss of eye vision [5].

Although monkeypox does not affect humans very often, the slight chance of affecting it should still make people think twice about their exposure to monkeys and rodents — especially in certain parts of the world where outbreaks of this disease happen more often. According to the Centers for Disease Control and Prevention (CDC), a new strain of monkeypox disease will infect millions globally in the coming years [6].

Monkeypox was initially found in 1958 and was rediscovered in the Republic of Congo in West Africa in 2014 [7]. While it may not be as well-known as the likes of Ebola or Zika, the monkeypox virus has the potential to become just as large of a global health threat as those two if enough is not done to stop it from spreading further. Recently, the virus has been slowly spreading, and the number of Monkeypox patients is increasing day by day. According to CDC, as of June 06, 2022, the virus had spread among 29 countries, and the number of Confirmed cases was around 1029 [8]. Currently, there are no appropriate treatments available for Monkeypox disease [9, 10]. However, two oral drugs, Brincidofovir and Tecovirimat, are recommended for urgent treatment, mainly used to treat the smallpox virus. Vaccination is the ultimate solution to prevent this disease [11].

The symptoms of Monkeypox, smallpox, and measles are almost similar making it difficult to identify without a proper laboratory test [12]. The definitive way to diagnose the virus is to use electronic microscopy and test the skin lesions. In addition, the virus can be identified using Polymerase chain reaction (PCR) testing, which is heavily used to test for COVID-19 [13]. PCR is usually used for laboratory tests. However, during the onset of COVID-19, we have seen that the PCR test kit cannot correctly diagnose COVID-19 patients around 40% of the time [14] which means that multiple tests are required to increase accuracy. As an effect, if Monkeypox becomes another global pandemic, then it will be hard to facilitate enough tool kits to test both Monkeypox and COVID-19 patients. Additionally, many developed nations cannot afford such an expensive tool kit to use regularly [15].

In recent past Machine learning (ML) demonstrated promising results in medical imaging and disease diagnosis [16] which means that diseases such as cancer, pneumonia, and COVID-19 can be detected without doctor intervention [17]. As Monkeypox symptoms significantly affect the human skin, images containing infected human skin can be used to develop ML-based diagnosis model [9].

Monkeypox disease detection using any ML or deep learning (DL) approach is not available at the time of writing. However, over the year, several studies demonstrated that DL-based models can be a reliable option to detect Chickenpox and Measles disease, which have almost similar symptoms as Monkeypox [18–20]. For example, Chae et al. (2018) employed a very deep neural network (DNN) and long-short term memory (LSTM) model to identify chickenpox, which outperforms the classic autoregressive integrated moving average (ARIMA) model [18]. Arias et al. (2020) developed a deep learning model to detect varicella-zoster, a virus that can cause damage to the eyes. Their proposed model can identify the virus up to 97% accuracy. Bhadula et al. (2019) employed convolutional neural networks (CNN) to detect skin disorders. The authors use the CNN model to detect acne and lichen planus and achieved 96% and 92% accuracy, respectively [20]. Sriwong et al. (2019) utilized the CNN approach to detect skin diseases and achieved 79.2% accuracy. Skin diseases such as actinic keratoses, basal cells, and benign keratosis are some of the skin diseases that the authors wanted to detect throughout the study [21].

Based on the referenced literature, it can be infer that, DL techniques have been used extensively to detect various skin diseases caused mainly by various infections. Therefore, traditional CNN is a good approach for developing deep learning-based models to diagnose the Monkeypox disease diagnosis. In this work, we proposed and tested six distinct improved deep CNN models by adopting models, namely, VGG16 [22], InceptionResNetV2 [23], ResNet50 [24–26], ResNet101 [27], MobileNetV2 [28], and VGG19 [22], using transfer learning approaches [29]. The following is a summary of our contribution:



Figure 1: Images retrieved from open source data repositories to use in our proposed research.

1. Improvement and assessment of six distinct deep learning models (VGG16, InceptionResNetV2, ResNet50, ResNet101, MobileNetV2, and VGG19) for detecting Monkeypox disease using image data.
2. Verify and interpret the model's performance employing Local Interpretable Model Agnostic Explanations (LIME).

## 2 Methodology

This study aims to detect Monkeypox disease by developing CNN model using transfer learning approaches. In this work, we have used pre-trained deep learning architectures to extract essential features that are practically difficult to initially identify by visual inspection due to their similarities with other infectious diseases such as chickenpox and measles. We then fed our data through several layers, where the top most dense layer is used to detect the Monkeypox disease.

### 2.1 Dataset

The traditional approach of deep learning demands a significant amount of input data in order to train. The recent advancement of transfer learning approaches, on the other hand, demonstrates that a limited dataset could be used to train and develop a robust CNN model that can efficiently perform during the predictions [14]. At the time of writing, only one publicly available dataset exists, which is obtained from the Kaggle repository. The assignment of the dataset that has been used during this study is presented in Table 1. Our assessment of the data size differs for two different studies. For Study One, we have used 76 samples (43 Monkeypox and 33 Non-Monkeypox images), whereas, for Study Two, 818 samples are used, which contains 587 Monkeypox and 231 Normal images. Figure 1 presents a set of

Table 1: Monkeypox datasets used in this study.

Dataset	Label	Train set	Test set	Total
Study One	Monkeypox	34	9	76
	Normal	26	7	
Study Two	Monkeypox	469	118	818
	Normal	185	46	

representative images of both Monkeypox and Non-Monkeypox individuals from the aforementioned datasets.

## 2.2 Data Augmentation

Data augmentation is a technique for increasing the size of a training dataset without acquiring new data from existing training data [30]. Many computer vision applications have benefited from Deep CNN, which is sensitive to large amounts of data to reduce overfitting. An overfitting network detects a function with a significant variance to estimate the training dataset accurately. Affine transformations, deformations, or geometric distortions are often used to enrich data and enlarge sample sizes for deep neural networks [31]. We have applied data augmentation to reduce the danger of overfitting, which involves random image alterations such as flipping, rotation height and weight shift, shearing, and zooming.

**Flipping:** Flipping is performed on each image inside the training set. Vertical flips capture a distinctive property of medical images: reflection invariance in the vertical direction. Vertical inversions may not always correlate to images that are input. For input images, only horizontal flips of the source images are used. In contrast, a vertical mass flip would still result in a considerable weight.

**Scaling:** Each I is scaled in either the x or y-axis; more precisely, affine transformation is used.  $A = \begin{pmatrix} s_x & 0 \\ 0 & s_y \end{pmatrix}$

**Rotations:** Rotations are performed using the affine transformation as well,  $A = \begin{pmatrix} \cos\theta & -\sin\theta \\ \sin\theta & \cos\theta \end{pmatrix}$ , where  $\theta$  is a value between 0 and 360 degrees.

**Shearing:** Shear angle in degrees in a counter-clockwise direction scaled by 0.2 which is represented by the following affine transformation,  $A = \begin{pmatrix} 1 & s \\ 0 & 1 \end{pmatrix}$ .  $s$  defines the amount that I is sheared, and it is in the range of [0, 0.2].

**Translation:** Simply moving the image on the X or Y axis is required for translation (or both). For example, it might be assumed that the image seems to have a black background outside its boundaries and translate the image accordingly. This enhancement can discover the vast majority of things anywhere inside the image. Thus, CNN is compelled to examine everywhere.

## 2.3 Transfer learning approaches

Recent research demonstrates the outstanding performance of deep CNN for the classification of image data with a high accuracy rate [14]. The development of deep CNN-based models that have established themselves as a promising tool for image classification and computer vision is gaining popularity day by day [32, 33]. Traditional CNN requires large amounts of data, whereas transfer learning can be applied to develop a model that can be adopted for other tasks [14]. During this study, the internal structure of the existing models was kept same to extract the important features from the Monkeypox images without further increasing any CNN-related complexity. Then the top most layers are modified to perform the classification. Throughout the course of this research, we modified six distinct deep-learning models, namely, VGG16, InceptionResNetV2, ResNet50, ResNet101, MobileNetV2, and VGG19.

Figure 3 displays the flow diagram of the proposed models used during this study.

## 2.4 Proposed architecture

A pre-trained network is one that has been trained on a large dataset and can be applied to other datasets with comparable properties. A prime example is VGG16 networks, which have been adopted by many recent literatures to detect COVID-19 during the onset of the COVID-19 pandemic [14, 34]. Figure 4 shows a sample modified architecture that has been proposed during this study for VGG16.

The modified architecture generally follows the following three steps:

1. The model is initially initialized with a pre-trained network without FC layers.
2. Then a new FC layer is added with "Softmax" activation function and added to the top of the actual VGG16 model.
3. Finally, during the training phase, the weight of the convolution is frozen so that the FC layer can be developed during the experiment.

Similar procedure is followed to develop every transfer learning model used during this study. In this study, the primary modification of the model for all CNN architecture is developed as shown in Figure 2.

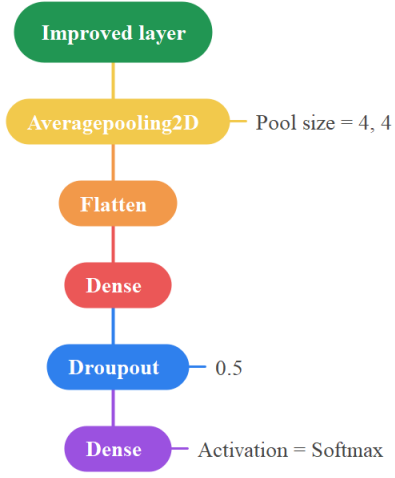


Figure 2: Modified layer

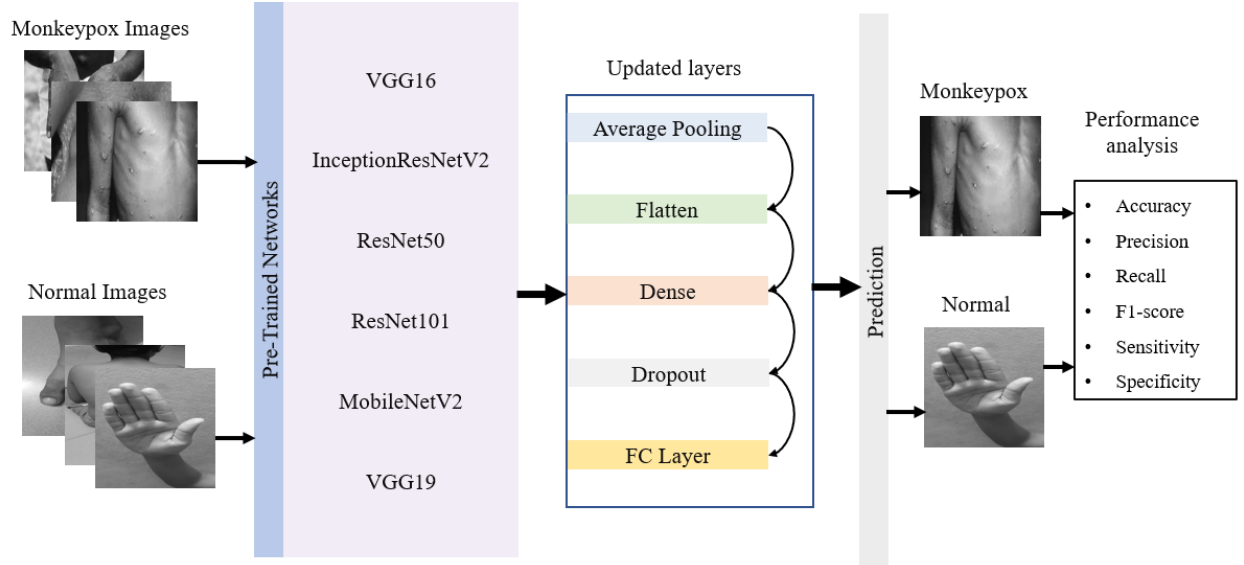


Figure 3: Flow diagram of the proposed models.

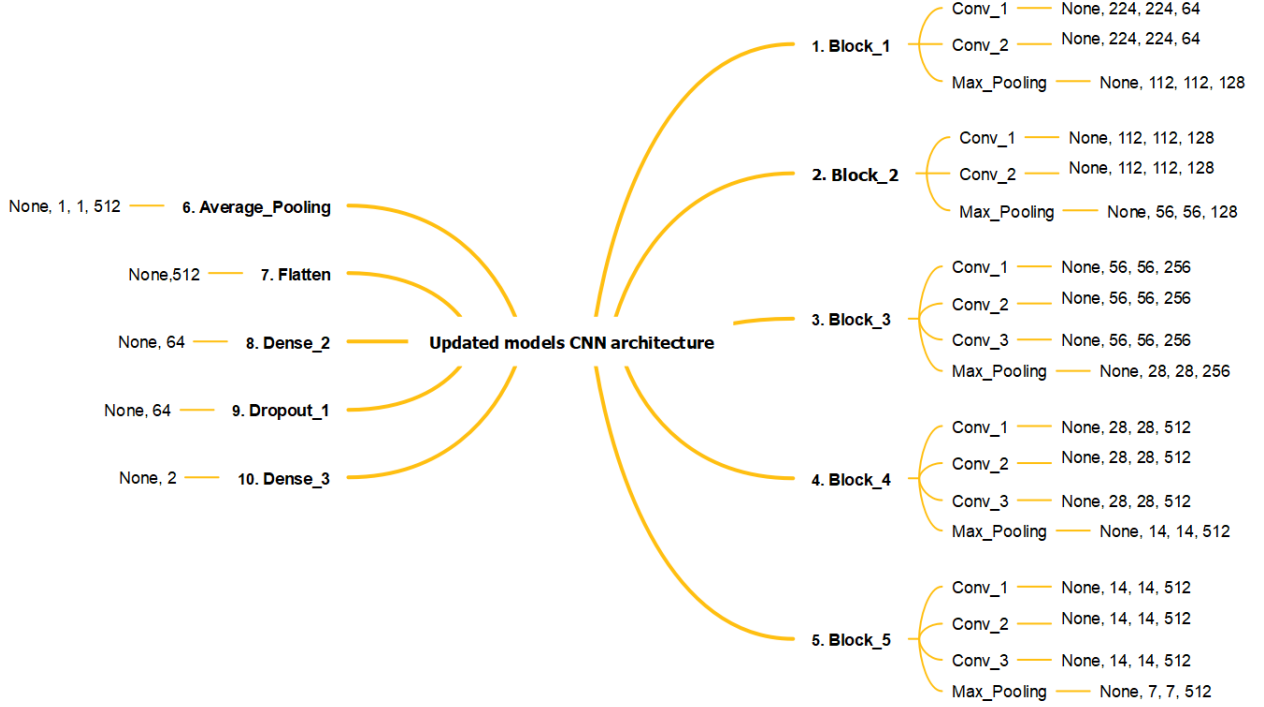


Figure 4: Updated VGG16 network implemented during this experiment.

Our proposed study optimized three parameters during the training phase: batch size, epochs, and learning rate. Manually tuning that parameter is time-consuming; therefore, we have used the grid search method to find the best results. Table 2 summarizes the initial and optimal parameters found during the experiment.

Table 2: Parameter settings used during this study.

Parameters	Study One		Study Two	
	Initial parameter	Optimize parameters	Initial parameters	Optimize parameters
Batch size	5, 10, 20, 40	10	10, 20, 30, 40	30
Epochs	20, 30, 40, 50	50	30, 40, 50, 70	50
Learning rate	.001, .01, 0.1	.001	.001, .01, 0.1	.001

## 2.5 Experiment setup

Adaptive momentum, also known as Adam, is employed to optimize the performance of our proposed model due to the fact that it has a reliable performance with regard to binary image classification [35]. The experiment was carried out using an office-grade laptop with a configuration of Windows 10, Core I7, and with 16 GB RAM facilities. The dataset is split into the following ratios, which is often common in machine learning domains—train set: test set= 80:20. The overall experimentation is run five times, and the final result is presented by averaging all five results. To evaluate the model’s performance following statistical measurement is used [32]:

$$Accuracy = \frac{T_p + T_n}{T_p + T_n + F_p + F_n} \quad (1)$$

$$Precision = \frac{T_p}{T_p + F_p} \quad (2)$$

$$Recall = \frac{T_p}{T_n + F_p} \quad (3)$$

$$F1 - score = 2 \times \frac{\text{Precision} \times \text{Recall}}{\text{Precision} + \text{Recall}} \quad (4)$$

$$\text{Sensitivity} = \frac{T_p}{T_p + F_n} \quad (5)$$

$$\text{Specificity} = \frac{T_n}{T_n + F_p} \quad (6)$$

Here,  $T_p$  (True Positive) = Monkeypox infected individual identified as Monkeypox

$T_n$  (True Negative) = Monkeypox infected individual identified as non-Monkeypox

$F_p$  (False Positive) = Non-Monkeypox individual identified as Monkeypox

$F_n$  (False Negative) = Monkeypox individual identified as non-Monkeypox.

### 3 Results

#### 3.1 Study One

Equations 1, 2, 3, 4, 5 and 6 were used in Study One to investigate each and every CNN models performance on both the train and test sets. In this particular scenario, InceptionResNetV2 and MobileNetV2 performed far better than any other models in terms of accuracy, precision, recall, F-1 score, sensitivity, and specificity (refer to Table 3). On the other hand, ResNet50 showed the worst performance out of all the measurements. The results of the performance of all

Table 3: Monkeypox prediction performance of all models on the training set using various statistical measurements for Study One.

Model	Performance					
	Accuracy	Precision	Recall	F1-Score	Sensitivity	Specificity
VGG16	0.98	0.98	0.98	0.98	1.0	0.96
InceptionResNetV2	1	1	1	1	1	1
ResNet50	0.56	0.32	0.57	0.41	1	0
ResNet101	0.68	0.80	0.68	0.63	1	0.26
MobileNetV2	1	1	1	1	1	1
VGG19	0.98	0.98	0.98	0.98	1	0.96

of the models with regard to the test set are presented in Table 4. While the models ResNet50 and ResNet101 showed the least performance, InceptionResNetV2 and VGG19 demonstrated the best performance across all criteria.

Table 4: Monkeypox prediction performance of all models on the testing set using various statistical measurements for Study One.

Model	Performance					
	Accuracy	Precision	Recall	F1-Score	Sensitivity	Specificity
VGG16	0.81	0.86	0.81	0.80	1	0.42
InceptionResNetV2	0.90	0.88	0.88	0.77	1	0.95
ResNet50	0.56	0.32	0.56	0.40	1	0
ResNet101	0.56	0.32	0.56	0.40	1	0
MobileNetV2	0.81	0.82	0.81	0.81	0.77	0.85
VGG19	0.93	0.94	0.94	0.94	1	0.85

### 3.2 Confusion matrix

The total prediction of the model can be represented using confusion matrices. Figure 5 illustrates the confusion matrices acquired for the train set during Study One. Both the InceptionResNetV2 and MobileNetV2 models accurately categorized all patients, as shown in the Figure 5. Contrary, VGG16, ResNet50, ResNet101 and VGG19 misclassified 1, 26, 19 and 1 patients respectively. As a result, we can draw the conclusion that the performance of the ResNet50 model is the worst among all of the models based on the assessment of the confusion matrices.

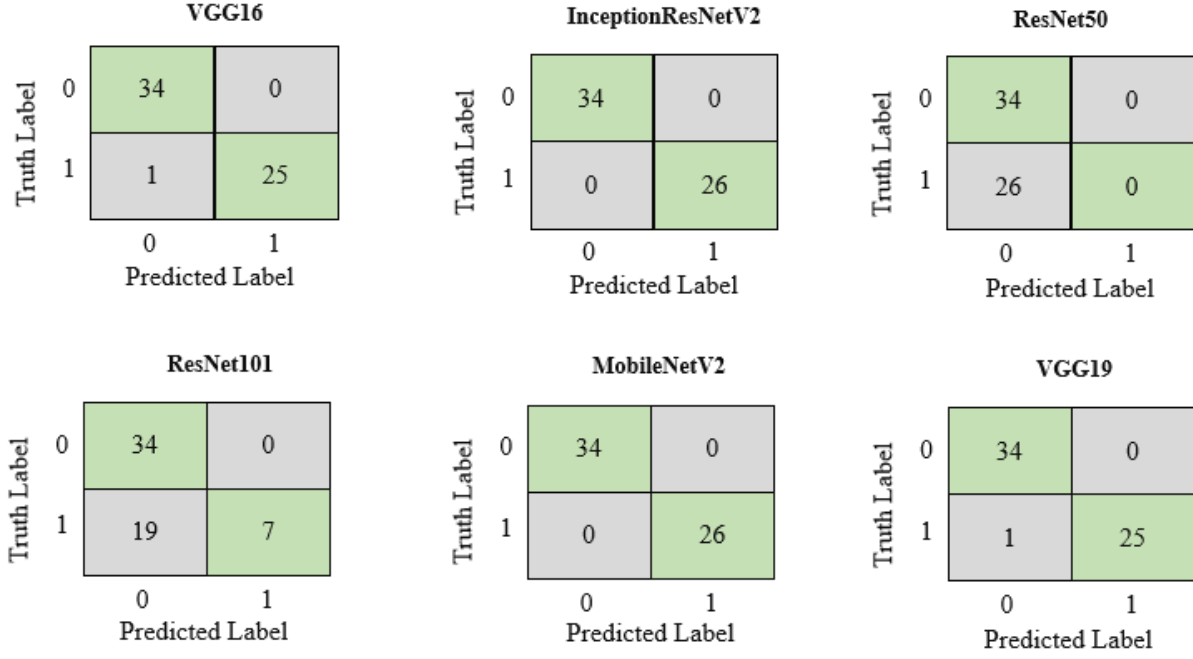


Figure 5: Study one confusion matrices for the train set.

Figure 6 displays the confusion matrices for Study One on the test set. Models InceptionResNetV2 displayed the best performance by misclassifying only two patients, while both ResNet50 and ResNet101 demonstrated the worst performance by misclassifying seven patients. Considering the performance on both the train and test set, it can be inferred that the performance of modified InceptionResNetV2 remains constant for both train and test set, ultimately demonstrated best performance compared to all other models.

### 3.3 Models' performance during training

Figure 7 shows train and test performance during each epoch for the CNN models used in this study. The figure shows that the model's performance during each epoch improves for InceptionResNetV2 and VGG19 until 50 epochs. On the other hand, ResNet50 and ResNet101's performance fluctuated during each epoch and overfitted at 50 epochs.

#### 3.3.1 Explainable AI with Lime

Figure 8 explains the model's prediction using LIME. The best performance was observed when LIME model is used with 150 perturbation. The difference between each perturbation was calculated by employing cosine metric with a kernel size of 0.2. A simple linear interpolation is used to provide the explanation of the models. Furthermore, the coefficient was calculated for each superpixel value. Finally, top four features are identified that potentially affect the model's prediction.



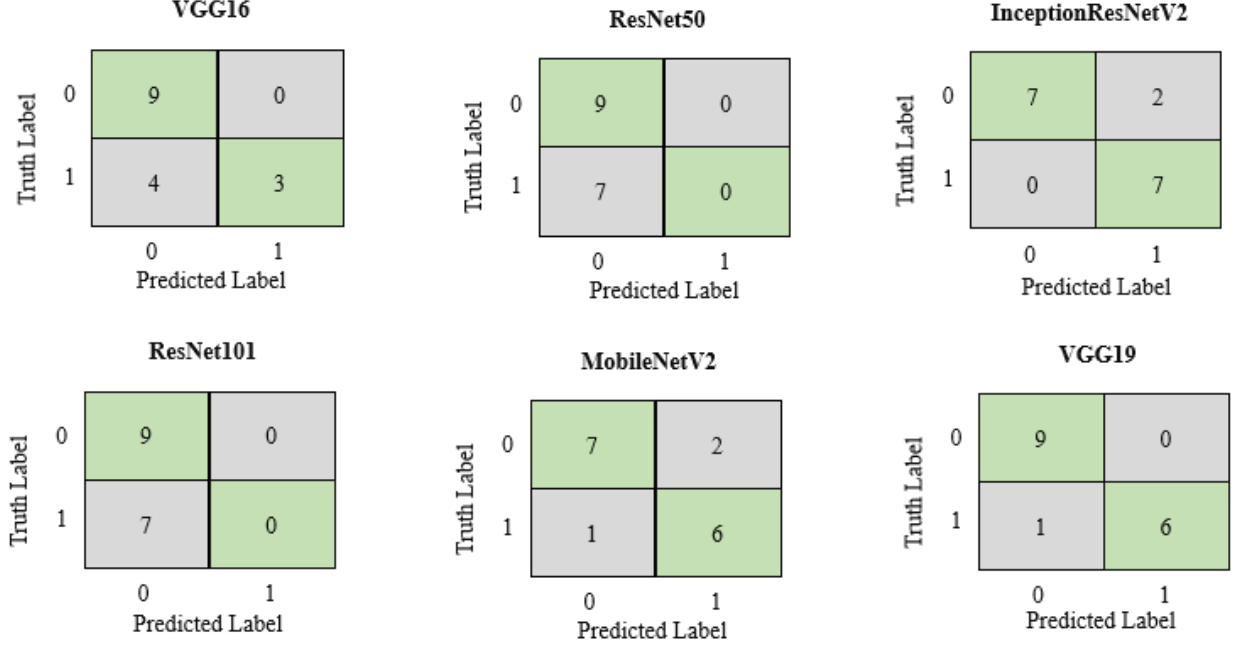


Figure 6: Study one confusion matrices for the test set.

### 3.4 Study Two

In Study Two, on the train set (refer to Table 5), InceptionResNetV2 and MobileNetV2 outperformed all other models across all measures, while ResNet50 and ResNet101 demonstrated the worst performance.

Table 5: Monkeypox prediction performance of all models on training set using various statistical measurements for Study Two.

Model	Performance					
	Accuracy	Precision	Recall	F1-Score	Sensitivity	Specificity
VGG16	0.97	0.98	0.97	0.98	0.99	0.94
InceptionResNetV2	1	1	1	1	1	1
ResNet50	0.72	0.51	0.72	0.6	1	0
ResNet101	0.72	0.36	0.50	0.42	1	0
MobileNetV2	1	1	1	1	1	1
VGG19	0.94	0.94	0.92	0.93	0.97	0.85

Table 6 shows the test performance of various models applied during study two as a transfer learning approach. The highest performance was observed for MobileNetV2, and the lowest performance was identified for ResNet101 across all measures.

#### 3.4.1 Confusion matrices

Figure 9 shows the confusion matrices for the train set during Study Two. Both the InceptionResNetV2 and MobileNetV2 accurately categorized all patients, as seen in the Figure 9. In contrast, VGG16, ResNet50, Resnet101 and VGG19 misclassified 15, 185, 185 and 39 patients respectively. As a result, we are able to draw the conclusion that the performance of the ResNet50 and ResNet101 models is the worst out of all of them based on the analysis of the confusion matrices.

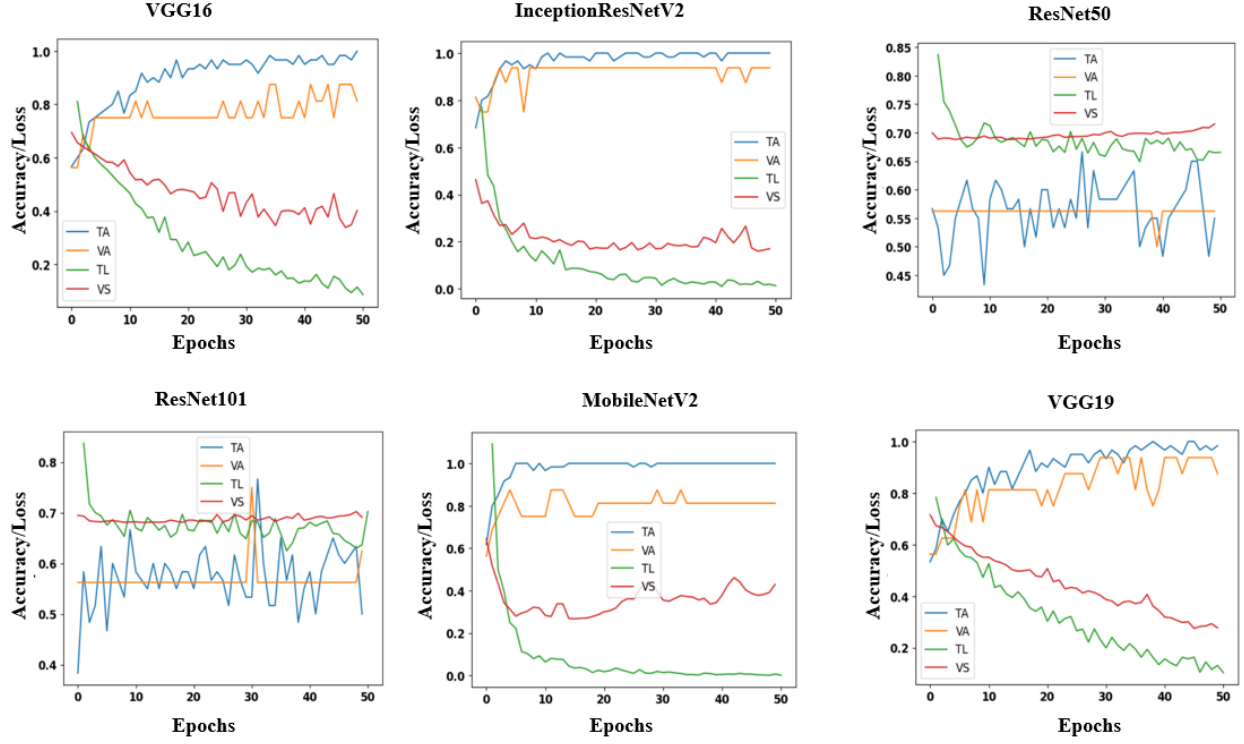


Figure 7: Modified models accuracy and loss during each epoch applied to Study One. TA—train accuracy, VA—validation accuracy, TL—train loss, VS—validation loss.

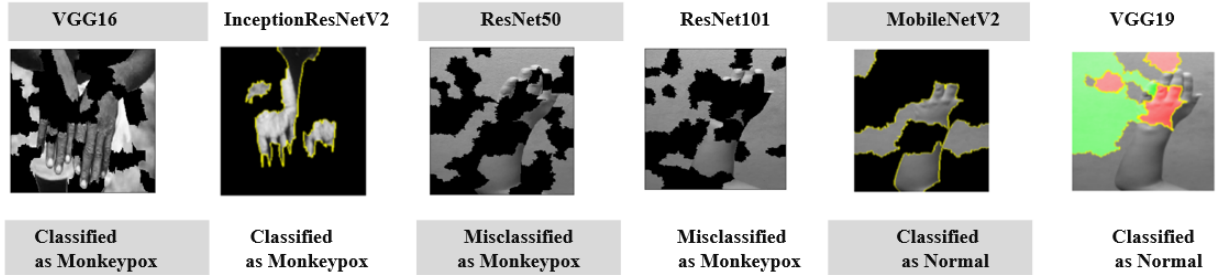


Figure 8: The top four features that facilitated the classification and misclassification of monkeypox patients from infected or non-infected images during Study One.

Figure 10 displays the confusion matrices for Study One on the test set. MobileNetV2 displayed the best performance by misclassifying only one patient, while ResNet50 and ResNet101 indicated the worst performance by misclassifying 46 patients. Considering both train and test analysis, it can be inferred that the best performance of modified MobileNetV2 remains constant for both train and test sets.

### 3.4.2 Models' performance during training

Figure 11 plotted train and test results during each epoch for all the CNN models for Study Two. The figure shows that the model's performance during each epoch shows better performance for most of the models except ResNet50 and ResNet101. The accuracy and loss for both the train and test set fluctuated and overfitted for models ResNet50 and ResNet101 after 25 epochs.

Table 6: Monkeypox prediction performance of all models on training set using various statistical measurements for Study Two.

Model	Performance					
	Accuracy	Precision	Recall	F1-Score	Sensitivity	Specificity
VGG16	0.93	0.93	0.90	0.91	0.97	0.82
InceptionResNetV2	0.98	0.98	0.97	0.98	0.99	0.95
ResNet50	0.72	0.51	0.72	0.6	1	0
ResNet101	0.72	0.36	0.50	0.42	1	0
MobileNetV2	0.99	0.99	0.99	0.99	1	0.97
VGG19	0.90	0.89	0.86	0.87	0.95	0.76

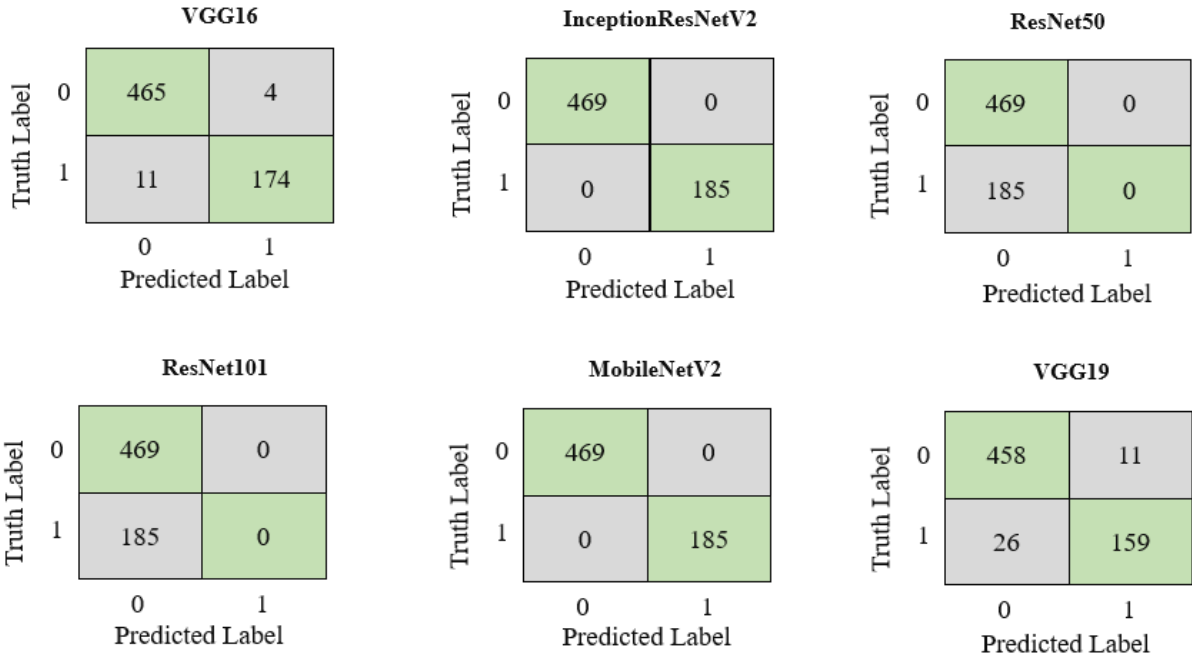


Figure 9: Study Two confusion matrices for the train set.

### 3.4.3 Explainable AI with Lime

The model's performance and explanation found in Study one align with Study Two. As shown in Figure 12, it is clear that ResNet50 and ResNet101 demonstrated the least performance by misclassifying Monkeypox patients.

## 4 Discussion

This study proposes and evaluates six distinct modified deep learning-based models in an effort to identify between patients with monkeypox and non-monkeypox symptoms. Our dataset contains limited samples, and we have further evaluated our model's accuracy with 95% confidence intervals inspired by referenced previous literature [19, 21, 34]. Table 7 shows model accuracy for Study One with 95% confidence intervals for the train and test set. Two approaches have been applied to measure the performance with CI: Wilson score and binomial proportional interval. As stated

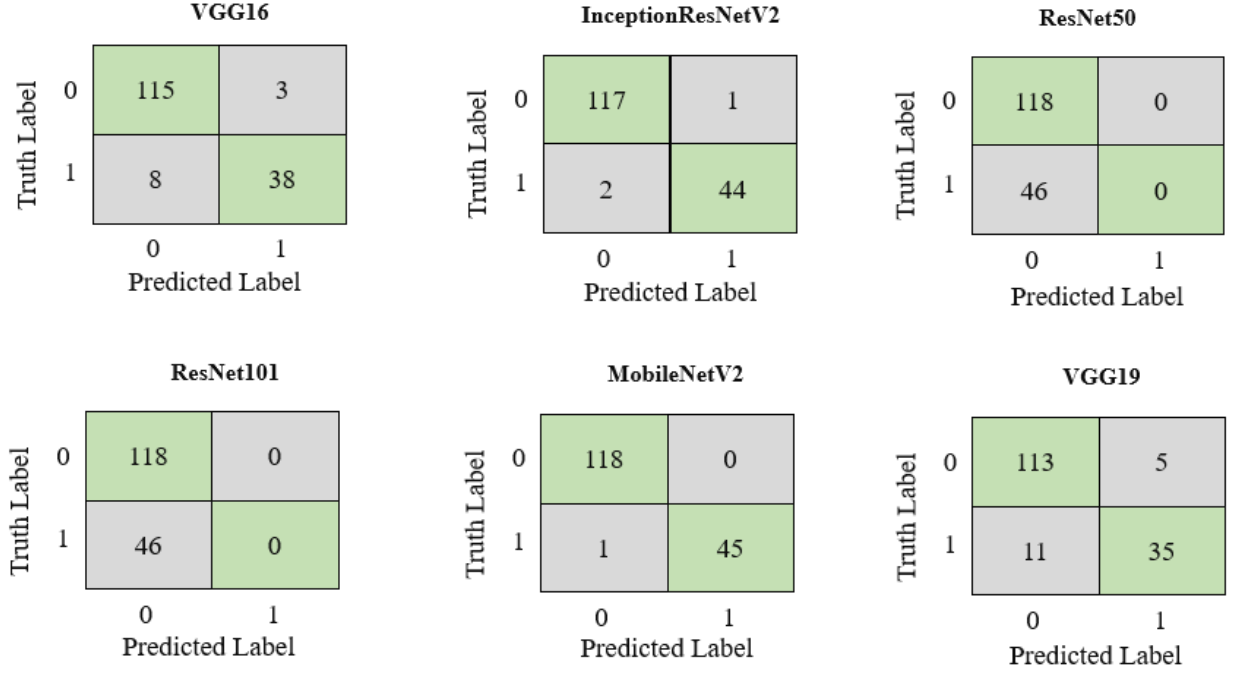


Figure 10: Study Two confusion matrices for the test set.

in Table 7, InceptionResNetV2 exceeded all other models in terms of accuracy. In contrast, ResNet50 demonstrates significantly lower performance on the train and test set while measuring the accuracy with CI.

Table 7: Confidence Interval ( $\alpha = 0.05$ ) of all models used in Study One in terms of accuracy.

Study One	Model	Train Accuracy	Methods	
			Wilson Score	Binomial proportion interval
Train set	VGG16	0.98	0.851-0.994	0.914-1.0
	InceptionResNetV2	1	0.93-0.99	1.00-1.00
	ResNet50	0.56	0.44-0.68	0.44-0.692
	ResNet101	0.68	0.55-0.78	0.56-0.80
	MobileNetV2	1	0.93-0.99	1.0-1.0
	VGG19	0.98	0.91-0.99	0.95-1.0
Test set	VGG16	0.81	0.56-0.93	0.62-1.0
	InceptionResNetV2	0.87	0.63-0.96	0.713-1.0
	ResNet50	0.56	0.33-0.76	0.32-0.81
	ResNet101	0.56	0.33-0.76	0.32-0.81
	MobileNetV2	0.81	0.56-0.93	0.62-1.0
	VGG19	0.93	0.71-0.98	0.81-1.0

Table 8 manifests the accuracy performance of six different models for Study Two. As stated in the table, MobileNetV2 outperformed all other models by showing better performance while ResNet50 and ResNet101 demonstrate the worst performance. Further, we have used Heatmap as a data visualization technique that demonstrates the phenomenon as color in two dimensions for different CNN layers during the prediction. Using heatmap, it is easy to identify the specific region where CNN establishes more focus during the prediction. The idea is to use the weights from the last dense layers and multiply them with the final CNN layer. In this work, we identify the potential Monkeypox infected areas using global average pooling (GAP). Class activation map (CAM) is initially used to collect each output of the

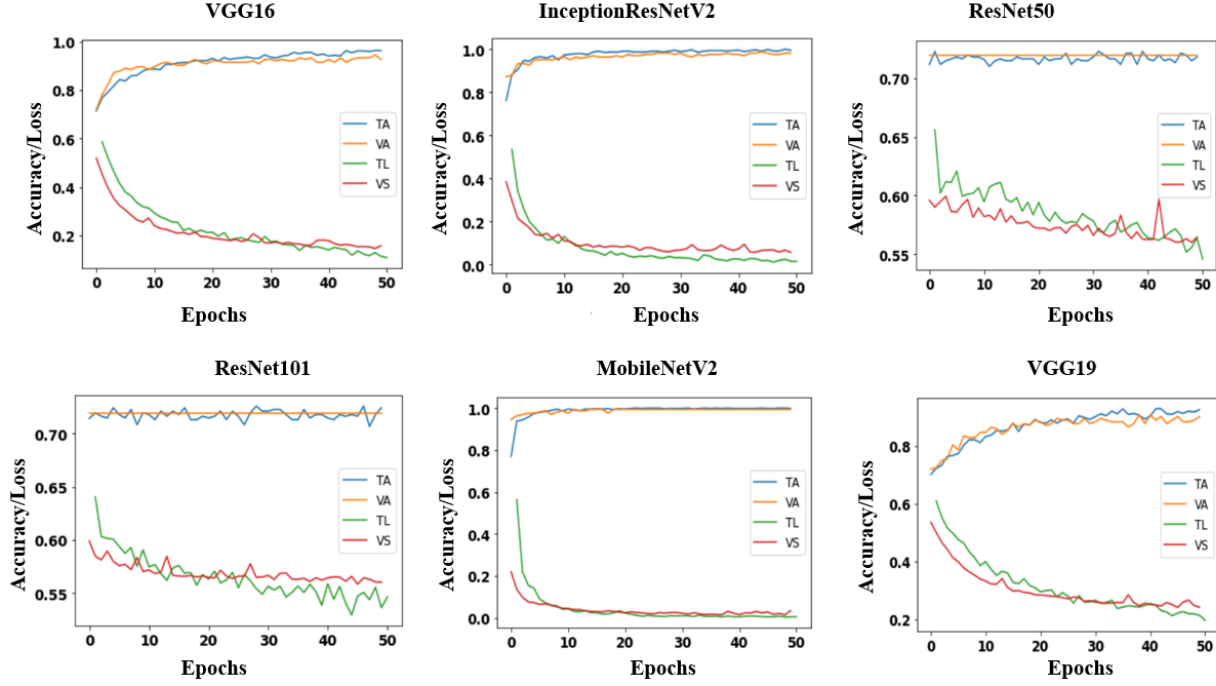


Figure 11: Modified models accuracy and loss during each epoch applied to Study Two. TA—train accuracy, VA—validation accuracy, TL—train loss, VS—validation loss

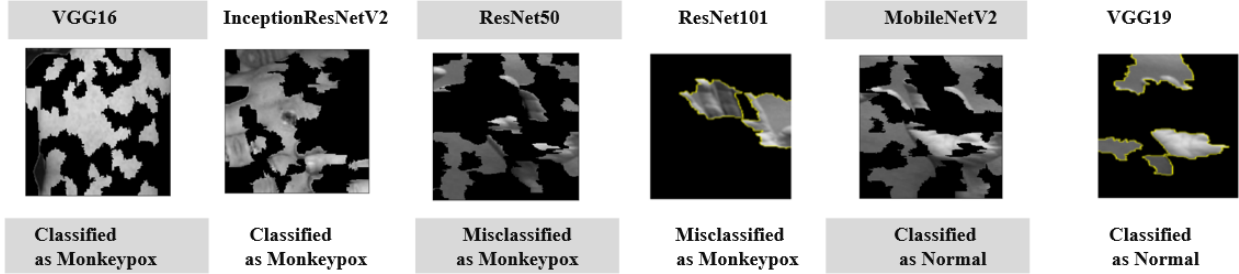


Figure 12: The top four features that facilitated the classification and misclassification of monkeypox patients from infected or non-infected hand images during Study Two.

convolutional layer and combine it in one shot. Figure 13(a) represents the spotted region by the ResNet50 models, whereas Figure 13(b) shows the heatmap on different spotted regions and Figure 13(c) on actual images. From the overall analysis across various measures, it can be inferred that MobileNetV2 and InceptionResNetV2 are the best models that can detect Monkeypox patients with perfect accuracy. It is relevant to emphasize that, at the time of experiment, there was no published or preprint literature where the transfer learning approach or deep learning approach was utilized to develop an AI-driven model to detect Monkeypox patients. Consequently, we could not evaluate our model's performance by comparing it with others' work. However, our higher performance results align with many referenced research, which established the potentiality of the transfer learning approach to develop image-based disease diagnosis. Examples include the InceptionResNetV2 model proposed by Narin et al. (2020), which trained with only 100 images to detect COVID-19 patients. Fujisawa et al. (2022) developed a deep learning-based model to detect skin tumors. The model was developed with 1842 patient data and achieved an accuracy of 76.5%. Our proposed model predictions are explained with LIME and further cross-checked by expert doctors' opinions. Our findings suggest that our modified MobileNetV2 and InceptionResNetV2 demonstrated a significant contribution to identifying the top feature that characterizes the onset of Monkeypox by identifying essential features from the images.

To further aid in comparing the model's final prediction with the visual evidence, we have also employed an image segmentation method to highlight highly infected areas. Figure 14 depicts the outcomes of threshold-based segmentation

Table 8: Confidence Interval ( $\alpha = 0.05$ ) of all models used in Study Two in terms of accuracy.

Study Two	Model	Train Accuracy	Methods	
			Wilson Score	Binomial proportion interval
Train set	VGG16	0.97	0.95-0.98	0.95-0.98
	InceptionResNetV2	1	0.99-1.0	1.0-1.0
	ResNet50	0.72	0.68-0.75	0.68-0.75
	ResNet101	0.72	0.68-0.75	0.68-0.75
	MobileNetV2	1	0.99-1.0	1.0-1.0
	VGG19	0.94	0.91-0.95	0.92-0.95
Test set	VGG16	0.93	0.88-0.96	0.89-0.97
	InceptionResNetV2	0.98	0.94-0.99	0.961-1.0
	ResNet50	0.72	0.68-0.75	0.68-0.75
	ResNet101	0.72	0.68-0.75	0.68-0.75
	MobileNetV2	0.99	0.96-0.99	0.98-1.0
	VGG19	0.90	0.84-0.93	0.85-0.94

applied to images of hands infected with the Monkeypox virus. The region of interest (ROI) has been defined using the pixel values of the infected areas. Then, a mask is generated for use in segmenting and generating the final output.

The major purpose of this research was to create a deep learning-based model capable of detecting patients with Monkeypox symptoms using a dataset of images of Monkeypox patients. Due to a lack of data, the scope of the current literature in this topic remains limited at this time. In the near future, it will be fascinating to examine how our suggested model performs on the multiclass and a large dataset.

## 5 Conclusion

This work proposed and tested six alternative modified deep learning models for detecting Monkeypox disease. We discovered that a modified MobileNetV2 and InceptionResNetV2 could identify between Monkeypox and Non-Monkeypox patients with an accuracy ranging from 90% to 100%. In addition to that, we have applied LIME, in order to comprehend and verify the predictions made by our model, demonstrating our suggested models' superiority in detecting Monkeypox illnesses. We expect that our study outcomes will provide future academics and practitioners some insight into the use of transfer learning models and explainable AI in constructing secure and trustworthy Monkeypox disease diagnosis models. The steps that are being used during this study will be considered in developing deep learning models using mixed data, evaluating the model's performance on the highly imbalanced dataset, creating fake samples using Generative adversarial networks (GAN), and developing a mobile-based user-friendly application that can be used to diagnose Monkeypox disease.

## References

- [1] Livia V Patrono, Kamilla Pléh, Liran Samuni, Markus Ulrich, Caroline Röthmeier, Andreas Sachse, Silvia Muschter, Andreas Nitsche, Emmanuel Couacy-Hymann, Christophe Boesch, et al. Monkeypox virus emergence in wild chimpanzees reveals distinct clinical outcomes and viral diversity. *Nature Microbiology*, 5(7):955–965, 2020.
- [2] Scott Parker, Anthony Nuara, R Mark L Buller, and Denise A Schultz. Human monkeypox: an emerging zoonotic disease. *Future Microbiology*, 2007.
- [3] Samson Wong, Susanna Lau, Patrick Woo, and Kwok-Yung Yuen. Bats as a continuing source of emerging infections in humans. *Reviews in medical virology*, 17(2):67–91, 2007.
- [4] Centers for Disease Control and Prevention. Monkeypox Signs and Symptoms., 2022. Last accessed May 30, 2022.
- [5] Mary G Reynolds, Andrea M McCollum, Beatrice Nguete, Robert Shongo Lushima, and Brett W Petersen. Improving the care and treatment of monkeypox patients in low-resource settings: applying evidence from contemporary biomedical and smallpox biodefense research. *Viruses*, 9(12):380, 2017.

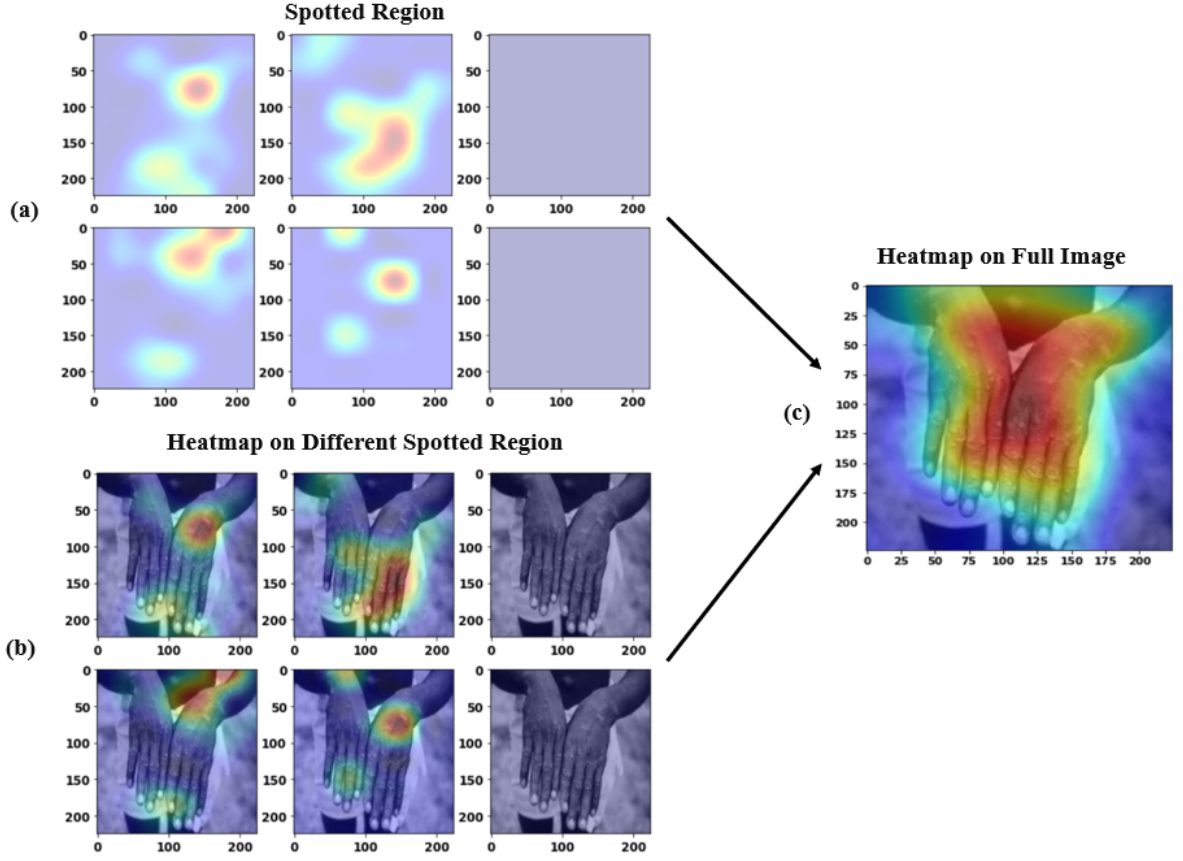


Figure 13: Heatmap of class activation on Monkeypox patient image.

- [6] Anthony S Fauci. Emerging and reemerging infectious diseases: the perpetual challenge. *Academic Medicine*, 80(12):1079–1085, 2005.
- [7] Michaelleen Doucleff. Scientists warned us about monkeypox in 1988. Here’s why they were right., 2022. Last accessed May 27, 2022.
- [8] Centers for Disease Control and Prevention. 2022 Monkeypox and Orthopoxvirus Outbreak Global Map., 2022. Last accessed June 07, 2022.
- [9] Md Manjurul Ahsan, Muhammad Ramiz Uddin, Mithila Farjana, Ahmed Nazmus Sakib, Khondhaker Al Momin, and Shahana Akter Luna. Image data collection and implementation of deep learning-based model in detecting monkeypox disease using modified vgg16. *arXiv preprint arXiv:2206.01862*, 2022.
- [10] Md Manjurul Ahsan, Muhammad Ramiz Uddin, and Shahana Akter Luna. Monkeypox image data collection. *arXiv preprint arXiv:2206.01774*, 2022.
- [11] Centers for Disease Control and Prevention. Monkeypox and Smallpox Vaccine., 2022. Last accessed May 30, 2022.
- [12] David L Heymann, Mark Szczeniowski, and Karin Esteves. Re-emergence of monkeypox in africa: a review of the past six years. *British medical bulletin*, 54(3):693–702, 1998.
- [13] Centers for Disease Control and Prevention. Diagnostic Tests., 2022. Last accessed May 30, 2022.
- [14] Md Manjurul Ahsan, Md Tanvir Ahad, Farzana Akter Soma, Shuva Paul, Ananna Chowdhury, Shahana Akter Luna, Munshi Md Shafwat Yazdan, Akhlaqur Rahman, Zahed Siddique, and Pedro Huebner. Detecting sars-cov-2 from chest x-ray using artificial intelligence. *Ieee Access*, 9:35501–35513, 2021.
- [15] Md Manjurul Ahsan, Tasfiq E. Alam, Theodore Trafalis, and Pedro Huebner. Deep mlp-cnn model using mixed-data to distinguish between covid-19 and non-covid-19 patients. *Symmetry*, 12(9):1526, 2020.



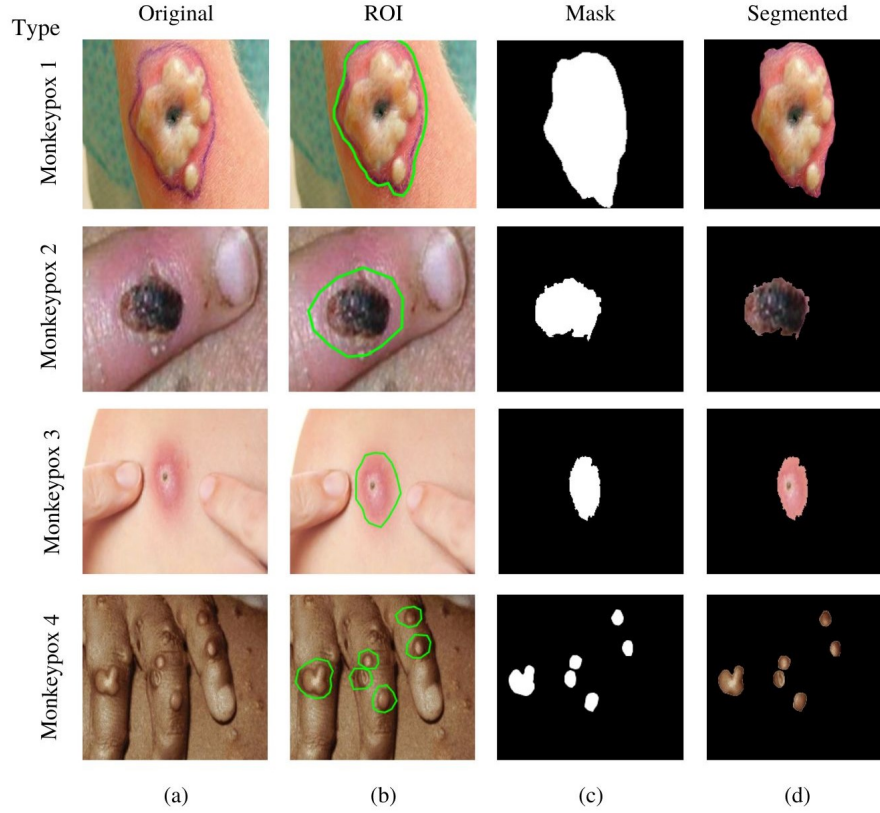


Figure 14: Threshold-based segmentation (a) Original, (b) ROI, (c) Mask, (d) Segmented

- [16] Md Manjurul Ahsan and Zahed Siddique. Machine learning-based heart disease diagnosis: A systematic literature review. *Artificial Intelligence in Medicine*, page 102289, 2022.
- [17] Md Manjurul Ahsan, Shahana Akter Luna, and Zahed Siddique. Machine-learning-based disease diagnosis: A comprehensive review. In *Healthcare*, volume 10, page 541. MDPI, 2022.
- [18] Sangwon Chae, Sungjun Kwon, and Donghyun Lee. Predicting infectious disease using deep learning and big data. *International journal of environmental research and public health*, 15(8):1596, 2018.
- [19] R Arias and J Mejía. Varicella zoster early detection with deep learning. In *2020 IEEE Engineering International Research Conference (EIRCON)*, pages 1–4. IEEE, 2020.
- [20] Shuchi Bhadula, Sachin Sharma, Piyush Juyal, and Chitransh Kulshrestha. Machine learning algorithms based skin disease detection. *International Journal of Innovative Technology and Exploring Engineering (IJITEE)*, 9(2), 2019.
- [21] Kittipat Sriwong, Supaporn Bunrit, Kittisak Kerdprasop, and Nittaya Kerdprasop. Dermatological classification using deep learning of skin image and patient background knowledge. *International Journal of Machine Learning and Computing*, 9(6):862–867, 2019.
- [22] Karen Simonyan and Andrew Zisserman. Very deep convolutional networks for large-scale image recognition. *arXiv preprint arXiv:1409.1556*, 2014.
- [23] Christian Szegedy, Sergey Ioffe, Vincent Vanhoucke, and Alexander A Alemi. Inception-v4, inception-resnet and the impact of residual connections on learning. In *Thirty-first AAAI conference on artificial intelligence*, page 4278–4284, 2017.
- [24] Takuya Akiba, Shuji Suzuki, and Keisuke Fukuda. Extremely large minibatch sgd: Training resnet-50 on imagenet in 15 minutes. *arXiv preprint arXiv:1711.04325*, 2017.
- [25] Warid Islam, Meredith Jones, Rowzat Faiz, Negar Sadeghipour, Yuchen Qiu, and Bin Zheng. Improving performance of breast lesion classification using a resnet50 model optimized with a novel attention mechanism. *Tomography*, 8(5):2411–2425, 2022.



- [26] Warid Islam, Gopichandh Danala, Huong Pham, and Bin Zheng. Improving the performance of computer-aided classification of breast lesions using a new feature fusion method. In *Medical Imaging 2022: Computer-Aided Diagnosis*, volume 12033, pages 84–91. SPIE, 2022.
- [27] Kaiming He, Xiangyu Zhang, Shaoqing Ren, and Jian Sun. Deep residual learning for image recognition. In *Proceedings of the IEEE conference on computer vision and pattern recognition*, pages 770–778, 2016.
- [28] Mark Sandler, Andrew Howard, Menglong Zhu, Andrey Zhmoginov, and Liang-Chieh Chen. Mobilenetv2: Inverted residuals and linear bottlenecks. In *Proceedings of the IEEE conference on computer vision and pattern recognition*, pages 4510–4520, 2018.
- [29] Meredith A Jones, Warid Islam, Rozwat Faiz, Xuxin Chen, and Bin Zheng. Applying artificial intelligence technology to assist with breast cancer diagnosis and prognosis prediction. *Frontiers in Oncology*, 12, 2022.
- [30] Md Shahin Ali, Md Sipon Miah, Jahurul Haque, Md Mahbubur Rahman, and Md Khairul Islam. An enhanced technique of skin cancer classification using deep convolutional neural network with transfer learning models. *Machine Learning with Applications*, 5:100036, 2021.
- [31] Arkadiusz Kwasigroch, Agnieszka Mikołajczyk, and Michał Grochowski. Deep neural networks approach to skin lesions classification—a comparative analysis. In *2017 22nd international conference on methods and models in automation and robotics (MMAR)*, pages 1069–1074. IEEE, 2017.
- [32] Md Manjurul Ahsan, Yueqing Li, Jing Zhang, Md Tanvir Ahad, Munshi Md Yazdan, et al. Face recognition in an unconstrained and real-time environment using novel bmc-lbph methods incorporates with dji vision sensor. *Journal of Sensor and Actuator Networks*, 9(4):54, 2020.
- [33] Md Manjurul Ahsan, Yueqing Li, Jing Zhang, Md Tanvir Ahad, and Kishor Datta Gupta. Evaluating the performance of eigenface, fisherface, and local binary pattern histogram-based facial recognition methods under various weather conditions. *Technologies*, 9(2):31, 2021.
- [34] Ali Narin, Ceren Kaya, and Ziynet Pamuk. Automatic detection of coronavirus disease (covid-19) using x-ray images and deep convolutional neural networks. *Pattern Analysis and Applications*, 24(3):1207–1220, 2021.
- [35] Alaa Ali Hameed, Bekir Karlik, and Mohammad Shukri Salman. Back-propagation algorithm with variable adaptive momentum. *Knowledge-Based Systems*, 114:79–87, 2016.